Effect of Parallel Diffusion of Equilibrium Pressure on Interaction between Interchange Mode and Static Magnetic Island*)

Kinya SAITO[1)], Katsuji ICHIGUCHI[1,2)] and Ryuichi ISHIZAKI[1,2)]

[1)]*The Graduate University for Advanced Studies, Toki 509-5292, Japan*

[2)]*National Institute for Fusion Science, Toki 509-5292, Japan*

(Received 6 December 2010 / Accepted 18 April 2011)

The effect of equilibrium pressure diffusion parallel to the magnetic field on the interaction between a resistive interchange mode and a static magnetic island is studied by means of a nonlinear numerical simulation based on the reduced magnetohydrodynamics equations. Previous work for the case without the parallel diffusion of the equilibrium pressure [K. Saito *et al.*, Phys. Plasmas **17**, 062504 (2010)] showed that two solutions exist for a given error magnetic field: one indicates the increase of the island width in the nonlinear evolution of the interchange mode and the other indicates the decrease of the width. For the case with parallel diffusion of the equilibrium pressure, our present study shows that only the solution indicating the increase of the width exists; we discuss the causes for this.

© *2011 The Japan Society of Plasma Science and Nuclear Fusion Research*

Keywords: static magnetic island, interchange mode, parallel diffusion of equilibrium pressure

DOI: 10.1585/pfr.6.2403072

1. Introduction

In the magnetic confinement of fusion plasmas, nested flux surfaces are desirable. However, error magnetic fields caused by the misalignment of the field coils and terrestrial magnetism can induce static magnetic islands. Such static islands can affect the plasma confinement. In the large helical device (LHD), it is able to control the static islands by using the local island diverter coils [1]. Change of the island size and the influence on the confinement are extensively studied in the experiments by utilizing the coils [2–4].

On the other hand, resistive interchange modes can be unstable in a heliotron device such as LHD because of the existence of a magnetic hill in the confinement region. Because the interchange mode also degrades the plasma confinement, it is crucial to study the linear stability and nonlinear dynamics of the mode. However, only a few studies [5–7] have performed direct numerical simulations of the static islands and interchange modes. Therefore, the interaction between static islands and interchange modes has not been studied adequately.

In this study, we analyze the direct interaction between a static island and an interchange mode, both of which have the same mode number, by following the nonlinear time evolution. A previous study [8] showed that two solutions exist for a given error field depending on the sign of the initial perturbations in the nonlinear saturation phase of the interchange mode. One solution corresponds to an increase in the island width and the other corresponds to a decrease in the island width. The study included the effect of the diffusion parallel to the magnetic field only for the perturbed pressure. To consider a more realistic situation, we include the effect of diffusion parallel to the magnetic field for the equilibrium pressure in this study. In this case, the term of the parallel diffusion of the equilibrium pressure in the equation of state automatically generates an initial perturbation. Therefore, the solution can be uniquely determined, and it corresponds to the increase or decrease of the island width. Hence, we focus on the change in the island width due to the nonlinear evolution of the interchange mode.

2. Model Equations and Calculation Conditions

The interaction between the interchange mode with $(m, n) = (1, 1)$ and the static island with the same mode number is studied using the reduced magnetohydrodynamics (MHD) equations [9]. These equations are suitable for the analysis of such low mode number physics. The reduced MHD equations are composed of Ohm's law, the vorticity equation and the equation of state for the poloidal flux Ψ, the stream function Φ and the pressure P. The normalized equations are given by

$$\frac{\partial \tilde{\Psi}}{\partial t} = -\boldsymbol{B} \cdot \nabla \tilde{\Phi} + \frac{1}{S} \tilde{J}_z, \tag{1}$$

$$\frac{\mathrm{d}\tilde{U}}{\mathrm{d}t} = -(\boldsymbol{B} \cdot \nabla \tilde{J}_z + \tilde{\boldsymbol{B}} \cdot \nabla J_{z\,\mathrm{eq}}) + \frac{\beta_0}{2\epsilon^2} \nabla \Omega_{\mathrm{eq}} \times \nabla \tilde{P} \cdot \hat{z} + \nu \nabla_\perp^2 \tilde{U}, \tag{2}$$

and

author's e-mail: saito.kinya@nifs.ac.jp

*) This article is based on the presentation at the 20th International Toki Conference (ITC20).

© 2011 The Japan Society of Plasma Science and Nuclear Fusion Research

$$\frac{\mathrm{d}\tilde{P}}{\mathrm{d}t} = (\hat{z}\times\nabla\tilde{\Phi})\cdot\nabla P_{\mathrm{eq}} + \kappa_{\perp}\nabla_{\perp}^2\tilde{P} + \kappa_{\parallel}(\boldsymbol{B}\cdot\nabla)(\boldsymbol{B}\cdot\nabla)(P_{\mathrm{eq}}+\tilde{P}), \quad (3)$$

respectively in the cylindrical coordinates (r,θ,z). The parallel diffusion term of equilibrium pressure,

$$Q = \kappa_{\parallel}(\boldsymbol{B}\cdot\nabla)(\boldsymbol{B}\cdot\nabla)P_{\mathrm{eq}}, \quad (4)$$

is involved in Eq. (3). These equations are solved using the NORM code [10]. The subscript 'eq' refers to the equilibrium quantity, and the tilde refers to the perturbed quantity. The magnetic field $\boldsymbol{B}$ is written as $\boldsymbol{B} = \boldsymbol{B}_{\mathrm{eq}} + \tilde{\boldsymbol{B}}$, where $\boldsymbol{B}_{\mathrm{eq}}$ and $\tilde{\boldsymbol{B}}$ are defined as $\boldsymbol{B}_{\mathrm{eq}} = \hat{z} + \hat{z}\times\nabla\Psi_{\mathrm{eq}}$ and $\tilde{\boldsymbol{B}} = \hat{z}\times\nabla\tilde{\Psi}$. Here, $\hat{z}$ denotes the unit vector in the z direction. The convective time derivative is given by $\mathrm{d}/\mathrm{d}t = \partial/\partial t + \tilde{\boldsymbol{v}}_{\perp}\cdot\nabla$, and the velocity $\tilde{\boldsymbol{v}}_{\perp}$ is given by $\tilde{\boldsymbol{v}}_{\perp} = \nabla_{\perp}\tilde{\Phi}\times\hat{z}$. The operator $\nabla_{\perp}$ is defined as $\nabla_{\perp} = \nabla - \hat{z}(\partial/\partial z)$. In addition, the current density in the z direction $\tilde{J}_z$ and the vorticity in the z direction $\tilde{U}$ are expressed as $\tilde{J}z = \nabla_{\perp}^2\tilde{\Psi}$ and $\tilde{U} = \nabla_{\perp}^2\tilde{\Phi}$, where $\nabla_{\perp}^2$ is given by $\nabla_{\perp}^2 = (1/r)(\partial/\partial r)(r\partial/\partial r) + (1/r^2)(\partial^2/\partial\theta^2)$. The dissipation parameters of $S, \nu, \kappa_{\perp}$, and $\kappa_{\parallel}$ are the magnetic Reynolds number, viscosity coefficient, perpendicular heat conductivity coefficient, and parallel heat conductivity coefficient, respectively. This analysis uses a large resistivity of $S = 10^4$ to enhance the influence of the interchange mode. Other parameters of $\nu = 1.5\times10^{-4}$, $\kappa_{\perp} = 1.0\times10^{-5}$, and $\kappa_{\parallel} = 1.0$ are used so that the $(m,n) = (1,1)$ component dominates.

Because we focus on the interaction between the interchange mode with $(m,n) = (1,1)$ and the static island with the same mode number, we assume that the perturbations have a single helicity with $n/m = 1/1$ as follows:

$$\tilde{\Psi}(r,\theta,z) = \sum_{n=0,m=n}^{N}\tilde{\Psi}_{m,n}, \quad \tilde{\Psi}_{m,n} = \Psi_{m,n}(r)\cos(m\theta - nz), \quad (5)$$

$$\tilde{\Phi}(r,\theta,z) = \sum_{n=0,m=n}^{N}\tilde{\Phi}_{m,n}, \quad \tilde{\Phi}_{m,n} = \Phi_{m,n}(r)\sin(m\theta - nz), \quad (6)$$

$$\tilde{P}(r,\theta,z) = \sum_{n=0,m=n}^{N}\tilde{P}_{m,n}, \quad \tilde{P}_{m,n} = P_{m,n}(r)\cos(m\theta - nz). \quad (7)$$

We employ $N = 30$ as the highest mode number. In this case, the kinetic energy E_K and the magnetic energy E_M are given by

$$E_K = \sum_{n=0,m=n}^{N}E_K^{m,n}, \quad E_K^{m,n} = \frac{1}{2}\int|\nabla_{\perp}\Phi_{m,n}\sin(m\theta - nz)|^2\mathrm{d}V, \quad (8)$$

$$E_M = \sum_{n=0,m=n}^{N}E_M^{m,n}, \quad E_M^{m,n} = \frac{1}{2}\int|\nabla_{\perp}\Psi_{m,n}\cos(m\theta - nz)|^2\mathrm{d}V. \quad (9)$$

The static magnetic island with $(m,n) = (1,1)$ is introduced by assuming that $\Psi_{1,1}$ has a finite value at the plasma boundary $(r = 1)$ [5–7],

$$\Psi_{1,1}(r=1) = \Psi_b, \quad (10)$$

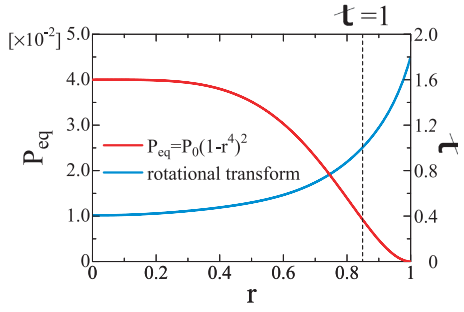

Fig. 1 Profiles of equilibrium pressure and rotational transform.

where Ψ_b is the external poloidal flux at the plasma boundary. Because the external field does not induce any current, the external poloidal flux satisfies the no-current condition $\nabla_{\perp}^2\tilde{\Psi}_{1,1} = 0$. The solution of this condition with the boundary condition given by Eq. (10) shows that the external poloidal flux corresponding to the static island with $(m,n) = (1,1)$ is given by $\Psi_{1,1} = \Psi_b r$.

We use a straight heliotron equilibrium corresponding to the LHD configuration with the vacuum magnetic axis located at 3.6 m [11]. The equilibrium is constructed by utilizing a three-dimensional equilibrium, which is calculated with the VMEC code [12] under the no-net-current and free-boundary conditions. We employ the equilibrium pressure profile of $P_{\mathrm{eq}} = P_0(1-r^4)^2$ with a beta value at the axis of $\beta_0 = 4\%$. Figure 1 shows the profiles of the equilibrium pressure P_{eq} and the rotational transform ι. The rational surface of $\iota = 1$ is located at $r = 0.85$, where a substantial pressure gradient exists to drive the interchange mode. The averaged field line curvature Ω_{eq} is calculated from the three-dimensional equilibrium magnetic field [13].

3. Island Evolution due to Interchange Mode

We follow the nonlinear evolution of the interchange mode with the static island by introducing finite Ψ_b. In this case, at the first time step of $t = \Delta t$, the parallel diffusion of the equilibrium pressure Q gives an initial perturbation of pressure P_b as given by

$$P_b = Q\Delta t|_{t=0} = -\kappa_{\parallel}(1-\iota)\Psi_b\frac{\mathrm{d}P_{\mathrm{eq}}}{\mathrm{d}r}\Delta t. \quad (11)$$

Therefore, any explicit external initial perturbation is not given.

Figure 2 shows the time evolution of the kinetic and magnetic energies of the interchange mode for $\Psi_b = 2.0\times10^{-3}$. A steady state is obtained after the nonlinear saturation of the interchange mode. As mentioned in Sec. 2, the $n = 1$ component dominates. The linearly growing phase does not appear for $\Psi_b = 2.0\times10^{-3}$, unlike the case without a static island. This difference arises because the inhomogeneous term Q is added continuously in Eq. (3). As shown in Eq. (4), the absolute value of $|Q|$ is decreased as

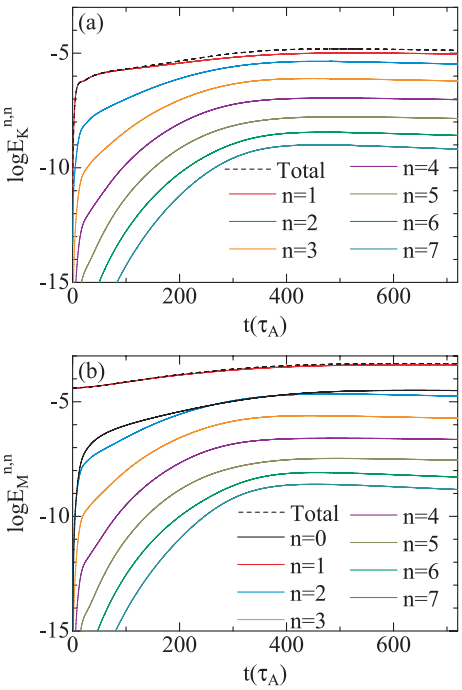

Fig. 2 Time evolution of (a) kinetic energy and (b) magnetic energy for $\Psi_b = 2.0 \times 10^{-3}$.

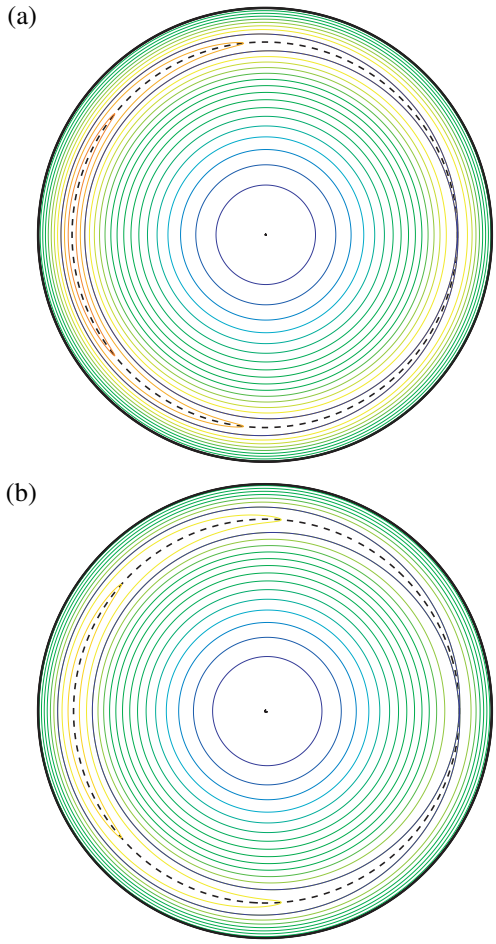

Fig. 3 Contours of the helical magnetic flux on the $z = 0$ poloidal cross section for $\Psi_b = 2.0 \times 10^{-3}$ at (a) $t = 0$ and (b) $t = 720\,\tau_A$.

$|\Psi_b|$. It is obtained that the linearly growing phase becomes seen explicitly as $|\Psi_b|$ is decreased.

To observe the change in the island due to the nonlinear saturation of the interchange mode, we plot the contours of the magnetic helical flux Ψ_h in Fig. 3, which is given by

$$\Psi_h(r,\theta,z) = \Psi_{\rm eq}(r) - \frac{1}{2}\frac{n}{m}r^2 + \tilde{\Psi}(r,\theta,z). \qquad (12)$$

Figure 3 shows the flux surfaces at $t = 0$ (before the growth of the interchange mode) and $t = 720\,\tau_A$ (after the nonlinear saturation of the mode). The island width is 0.105 at $t = 0$ and 0.153 at $t = 720\,\tau_A$. Figure 4 shows the dependence of the island width on Ψ_b. The sign of the island width indicates the island phase. A positive sign corresponds to islands with X-point at $\theta = 0$ and O-point at $\theta = \pi$. A negative sign corresponds to islands with X-point at $\theta = \pi$ and O-point at $\theta = 0$. The blue line shows the island width at $t = 0$, which is obtained by the analytical expression

$$w_B = 4\Psi_{m,n}\sqrt{\frac{1}{mr|\Psi_{m,n}|'}}\Bigg|_{r=r_s}, \qquad (13)$$

where r_s denotes the position of the resonant surface. The agreement between w_B and the island width determined by the Ψ_h contour was confirmed in Ref. [8]. The red circles show the island width after saturation of the interchange mode for each Ψ_b. For finite Ψ_b, the island width after saturation is always larger than that at $t = 0$. That is, the island width increases because of the nonlinear evolution

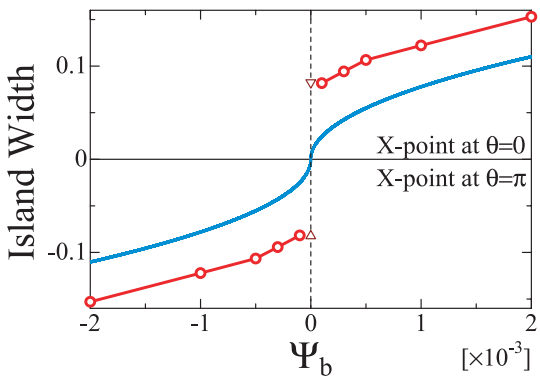

Fig. 4 Dependence of the island width on Ψ_b. The blue line shows the width at $t = 0$ evaluated with the analytic expression in Eq. (13). The triangles and circles show the width in the saturation of interchange mode for $\Psi_b = 0$ and finite values of Ψ_b, respectively.

of the interchange mode. The phase of the island is not changed by the mode. This property is independent of the sign of Ψ_b.

The island width after nonlinear saturation increases

with $|\Psi_b|$. However, the increment of the island width due to the interchange mode is almost independent of $|\Psi_b|$. This is attributed to the fact that the increase of the island width after saturation is mainly caused by the increase of the static island width.

4. Mechanism of Increase of Island Width

Here, we discuss the reason why the island width increases due to the interchange mode for the case with parallel diffusion of equilibrium pressure. For this purpose, we consider the properties of the mode structures of the interchange mode for the case with $\Psi_b = 0$ at first. In this case, P_b given by Eq. (11) is zero. Therefore, in the case without external initial perturbations, nothing happens. Thus, we employ a pressure perturbation given by

$$P_{\rm ini} = \sigma f(r), \tag{14}$$

as the initial perturbation for the calculation. Here, $f(r)$ is a function with a very small absolute value defined as

$$f(r) = \beta_0 10^{-18}\left\{1 - 4\left(r - \frac{1}{2}\right)^2\right\}^2, \tag{15}$$

and σ denotes the sign of the initial perturbation($\sigma = -1$ or $+1$). In this case, two solutions exist with the same absolute value and a different sign depending on the value of σ, as shown in Figs. 4 and 5.

Equation (14) and Fig. 5 show that the signs of the initial and saturation values of $P_{1,1}(r_m)$, where r_m denotes the position where the saturated $P_{1,1}$ has the maximum absolute value, are positive for $\sigma = +1$ and negative for $\sigma = -1$. That is, the sign of the saturated $P_{1,1}(r_m)$ is determined by that of $P_{\rm ini}$. This is because the function of $P_{\rm ini}$ involves a component that grows to the saturated $P_{1,1}$, and therefore the sign of the component is succeeded to the saturated $P_{1,1}$. Even in the case of $\Psi_b = 0$, $\Psi_{1,1}$ has a significant value at $r = r_s$, because a large resistivity of $S = 10^4$ and the cylindrical geometry are employed. Figure 5 also shows that the signs of $\Psi_{1,1}(r_s)$ and $P_{1,1}(r_m)$ are the same in the saturation of the interchange mode for either value of σ. Note that $r_m < r_s$.

We use this property of the interchange mode to analyze the case of finite Ψ_b. In this case, $P_{\rm ini}$ is given by P_b instead of Eq. (14). Figure 6 (a) shows the profile of P_b and the saturated $P_{1,1}$ for $\Psi_b = 2.0 \times 10^{-3}$. The profile of P_b is positive for $r < r_s$. Therefore, $P_{1,1}$ grows so as to be positive at $r = r_m$. Figure 6(b) shows the initial and saturated profiles of $\Psi_{1,1}$. At $t = 0$, $\Psi_{1,1}$ already has a positive value at $r = r_s$ because $\Psi_{1,1}$ is given by $\Psi_b r_s$ for positive Ψ_b. The change of $\Psi_{1,1}(r_s)$ due to the interchange mode is also positive because $P_{1,1}(r_m) > 0$. As a result, the absolute value of $\Psi_{1,1}(r_s)$ increases as the mode grows. This implies that the island width increases because it is proportional to the square root of $|\Psi_{1,1}(r_s)|$. The same result is obtained for the case of negative Ψ_b.

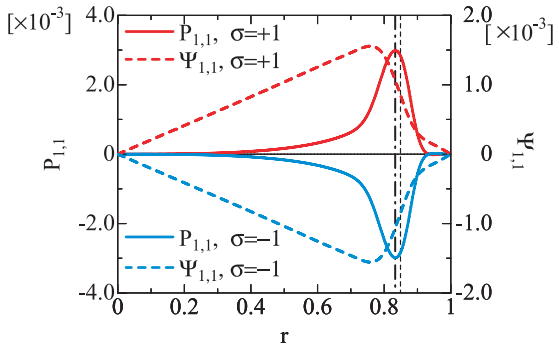

Fig. 5 Profiles of $P_{1,1}$ and $\Psi_{1,1}$ for $\Psi_b = 0$ in the saturation phase of the interchange mode. The dashed and dot-dashed lines indicate the positions of $r = r_s$ and $r = r_m$, respectively.

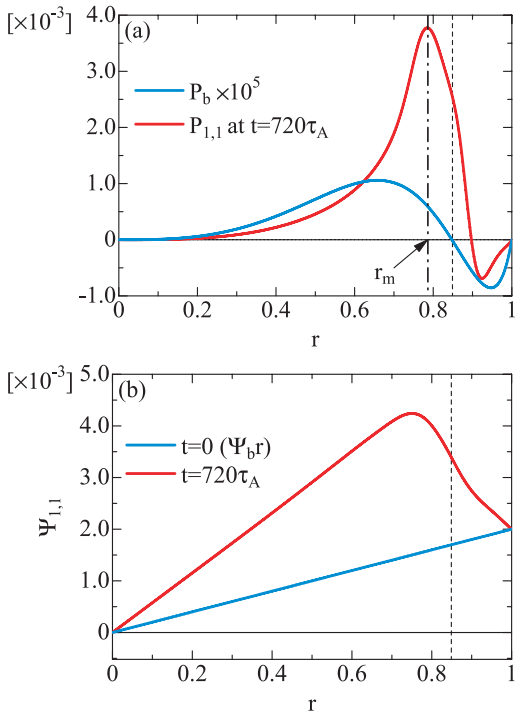

Fig. 6 Profiles of (a) $P_b \times 10^5$ and $P_{1,1}$ at $t = 720\,\tau_A$ and (b) $\Psi_{1,1}$ at $t = 0$ and $t = 720\,\tau_A$. The dashed and dot-dashed lines indicate the positions of $r = r_s$, and $r = r_m$, respectively.

5. Conclusions

The effect of equilibrium pressure diffusion parallel to the magnetic field on the interaction between a static island and an interchange mode is studied by following the nonlinear time evolution of the interchange mode in the straight LHD configuration.

A qualitative difference exists between the change of the island width for the cases with and without parallel diffusion of the equilibrium pressure. Only the saturation solution indicating the increase of the island width is obtained for the case with parallel diffusion of the equilibrium pressure; however, two solutions corresponding to the increase and decrease of the island width are obtained for

the case without. This results from the fact that the parallel diffusion term generating a pressure component that increases the poloidal flux at the resonant surface.

We use single helicity perturbations because we focus on the direct interaction between the interchange mode with $(m, n) = (1, 1)$ and the static island with the same mode number. When multiple helicity perturbations are employed, the excitations of the interchange modes at rational surfaces different from the island surface must be considered. If such modes grow substantially, they can interact with the island indirectly through the change in the structure of the magnetic field and the pressure profile. Incorporating this effect is beyond the scope of the present study, but it would be treated in a future work.

Acknowledgments

This work is partly supported by budget NIFS10 KLDT005 of the National Institute for Fusion Science and by a Grant-in-Aid for Scientific Research (C) 22560822 from JSPS, Japan.

[1] N. Ohyabu *et al.*, J. Nucl. Mater. **266-269**, 302 (1999).
[2] N. Ohyabu *et al.*, Plasma Phys. Control. Fusion **47**, 1431 (2005).
[3] Y. Narushima *et al.*, Nucl. Fusion **48**, 075010 (2008).
[4] F. Watanabe *et al.*, Nucl. Fusion **48**, 024010 (2008).
[5] T. Unemura *et al.*, Phys. Plasmas **11**, 1545 (2004).
[6] L. Garcia *et al.*, Phys. Plasma **8**, 4111 (2001).
[7] L. Garcia *et al.*, Nucl. Fusion **43**, 553 (2003).
[8] K. Saito *et al.*, Phys. Plasmas **17**, 062504 (2010).
[9] H. Strauss, Plasma Phys. **22**, 733 (1980).
[10] K. Ichiguchi *et al.*, Nucl. Fusion **43**, 1101 (2003).
[11] A. Komori *et al.*, Proc. 22th Fusion Energy Conf. OV/2-4 (2008).
[12] S. P. Hirshman *et al.*, Comput. Phys. Commun. **43**, 143 (1986).
[13] Y. Nakamura *et al.*, J. Comput. Phys. **128**, 43 (1996).